JOURNAL OF OPTOELECTRONICS AND ADVANCED MATERIALS, Vol. 10, No. 9, September 2008, p. 2474 - 2481

Light scattering measurement of nanoparticle aggregates by Scanning Flow Cytometer

R. FANTONI, L. FIORANI, A. PALUCCI, K. A. SEMYANOV[a], V. SPIZZICHINO
Laser Applications Section, ENEA, Via E.Fermi 45, 00044 Frascati, Italy
[a]*Institute of Chemical Kinetics and Combustion, Siberian Branch of Russian Academy of Sciences, Institutskaya 3, 630090 Novosibirsk, Russia*

Light scattering of nanoparticle aggregates has been measured by a Laser Scanning Flow Cytometer (LSFC) equipped with two channels: one for particles Side SCattering (SSC) detection and the other for measurements of the light scattered within an azimuth solid angle in the range 10°-70° (Light Scattering Pattern, LSP). By studying in particular SiC nanostructures we demonstrate the ability of the developed LSFC apparatus to dimensionally characterize and classify non spherical sub-micron particles. This is possible thanks to its unique property to analyze with a high rate singular particles in suspension and to retrieve their scattering pattern in a wide angular range. Measurements of the SSC and LSP of polystyrene microspheres have been performed to obtain empirical relationships between the LSP integral and particle size. Simulations on nanoparticle aggregate models have been carried out by the Discrete Dipole Approximation (DDA) method. The so obtained forward light scattering pattern for modeled structures has been compared to the experimental results. Moreover, DLS (Dynamic Light Scattering) measurements on the same samples have been performed to compare their data on size distribution to ones deriving from cytometer measurements. The comparison between DLS results and those obtained by the LSFC highlights advantages and limits of the two techniques versus the specific type of particles here studied.

(Received July 4, 2008; accepted August 14, 2008)

Keywords: Nanoparticle, Aggregate, Scanning flow cytometer, Light scattering

1. Introduction

The LSFC [1] (Laser Scanning Flow Cytometer) is here proposed as a new technique to measure concentration and size distribution of submicron aggregates of nanoparticles, in particular of SiC nanostructures. LSFC here presented is an evolution of the classical LFC [2] (Laser Flow Cytometer) thus allowing us to retrieve morphological and dimensional information of the target particles thanks to its ability to simultaneously measure side scattering (SSC) at 90° and light scattering pattern (LSP) in all the azimuthal angle φ and in a wide range of the polar angle θ, between 10° and 70°. Measurements of the LSP lead to morphological characterization of the particles under study by a parametric solution of the inverse light scattering problem (ILSP) [3].

In general classical flow cytometry is employed to evaluate properties of biological cells, characterized by a mean size between 1 and 10 μm. It can analyze them individually thanks to a hydrofocusing system that delivers them to the testing zone [2]. In usual LFC, the particle flow and the laser beam are orthogonally directed. When a particle crosses the beam, the radiation is scattered with an angular distribution that depends on size and refractive index. In general, in the commercial systems only the forward scattering (FSC) and the side scattering are measured. Although these are based on simplifications of the Mie theory and cannot retrieve size and refractive index, their approach allows the fast classification of cells in clinical field [4].

So far also LSFC has been used to characterize overall biological and biochemical samples and only a few papers deal with characterization of submicron particles [5, 6, 7]. A parametric solution of the ILSP has been developed and it can allow a determination of size and refractive index for spherically modeled particles over a range from 1 μm to 15 μm and from 1.37 to 1.6, respectively [3]. To our knowledge, until now only a modification of such method has been performed for submicron particles in the range of 0.5 μm to 1 μm [8].

In this work we have tried to develop a method to characterize, from the point of view of the size and morphology, structures, with a mean diameter smaller than 0.5 μm, that are becoming more and more important in the field of the nanotechnologies: aggregates of nanoparticles.

Nowadays, aggregates of nanoparticles are low cost nanostructures, since their formation is a common result of the entire formation process of nanoparticles [9], and they are proved to be very useful basic units for nanotechnology. Aggregates, actually, may be useful for their effects on surrounding materials or surfaces, enhancing their properties. Moreover aggregates can be valuable in the assembly of nanoporous layers and in nanolithography [10].

Their relevance suggests the need of more and more efficient and reliable methods to evaluate size and shape of such structures.

The composition and morphology of the nanopowders are, usually, investigated by methods suitable to evaluate crystalline structure and dimension, specific surface, powder dispersibility in liquids and agglomeration status, based on electron microscopy and X-Ray diffraction [9, 11]. Also the Dynamic Light Scattering (DLS) technique [12], based on the detection of the light scattered by particles or aggregates, is frequently employed in this field. These techniques are, however, not able to retrieve data on singular structures and provide fast statistics on a large amount of particles as LSFC can do.

Table 1. Data from certification and retrieved from empirical equation (eq. 7) for 0.2 and 0.5 μm polystyrene microspheres.

Microsphere	Number	Mol. Pr. size [μm]		LSFC size [μm]	
		Mean	SD	Mean	SD
0.2	1431	0.21	~ 0.01	0.24	0.02
0.5	801	0.50	~ 0.05	0.51	0.05

Here, starting from the investigation of polystyrene spheres, a method for individual submicron spherical particle size determination by a parametric solution of the ILSP has been tested. This theoretical approach is based on the development of approximated equations that relate the particle size to the parameters of the LSP thus allowing the real-time determination of particle size ranging from 0.2 μm to 1.0 μm.

Moreover, three-dimensional models of aggregates have been built and used for light scattering simulation performed with the Discrete Dipole Approximation (DDA) method. In this way we could compare LSFC experimental results on LSP to ones deriving from theory.

In order to compare the LSFC results with ones from a more conventional technique, DLS measurements on the same samples studied by cytometer have been performed. Size distributions obtained by these two methods have been compared and their advantages and limits versus the specific type of particles here investigated have been highlighted.

2. Materials and methods

2.1 LSFC experimental apparatus

Laser Flow Cytometry (LFC) technique enables us to determine different physical chemical features of single particles in solution as they flow in a fluid stream through a laser beam. The measured signals are, usually, light side scattering and fluorescence intensities [2]. The Scanning LFC (LSFC) is an improvement of the LFC with the main advantage of measuring light scattering in a very wide angle, instead of two preselected angles as in ordinary LFC. This feature allows a better morphological characterization of analyzed particles [13]. LSFC provides measurement of the forward light scattering pattern signal $I_{LSP}^{\exp}(\theta)$ in all the solid angle in the range 5° < θ < 100° (where θ is the polar scattering angle with respect to the flow direction) and the side scattering signal.

The experimental apparatus here used is shown in fig. 1. In this scheme D represents a diode laser working at 405 nm with a high polarization ratio (100:1). The large power (50 mW) of such source that allows the system to have good sensitivity, is combined with its short wavelength, necessary for the detection of sub-micrometric particles. The polarization ratio is increased by the Glan-Taylor polarizer P (extinction ratio: 100,000:1). The zero order quarter waveplate Q consents to switch from linear to circular polarization. Successively, after been focused by the plano-convex lens L (f: 60 mm) and having passed through the broadband dielectric mirror with a hole M, the beam coaxially impinges on a flow of particles in liquid suspension that gets across the capillary (diameter: 254 μm) of the cuvette C (sample IN). A hydrodynamic system of focusing assures the centrality of the sample flow inside the capillary. The optical cell (in quartz) is provided of a spherical mirror on the bottom. In the interaction region (length less than 5 mm) the beam has a small cross section (diameter around 30 μm FWHM) and thus the radiant energy flow is high.

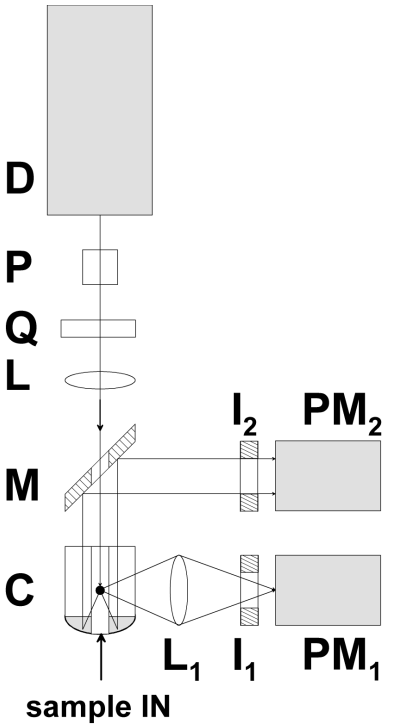

Fig. 1. Optical layout of LSFC apparatus used.

A photomultiplier, PM_1, detects the side scattering produced by the particle invested by the laser beam and collected by means of the objective L_1 (×50, NA: 0.30). The forward scattered light is reflected by the spherical reflector surface at the bottom of the cuvette, then it is

reflected by the mirror M and focused into the continuously variable iris diaphragm (∅: 0.8 mm) I_2 in front of the photomultiplier tube PM_2.

It has to be pointed out that for each position of the particle, within the sensing zone, there is a specific light scattering polar angle θ for which every ray scattered is reflected in parallel to the stream axis by the spherical mirror. Only these parallel rays are detected. Consequently, it is possible to determine the scattering intensity as a function of the polar angle in a wide interval of θ. In fact, this can be done by retrieving the position from the acquisition time of the signal, thanks to the measurement of the particle velocity and its transit time in a known point (detected by the side scattering).

2.2 Theoretical approach

From the quantities measured by the experimental apparatus, i.e. the light scattering pattern and the side scattering signals, the elements of the Mueller matrix associated to the particle responsible for the light scattering can be evaluated [14].

Using the Mueller formalism, the matrix elements combination measurable by the optical set-up of the LSFC presented in fig.1 can be expressed as follows:

$$\left[S_{11}(\theta,\phi)+S_{14}(\theta,\phi)\right] \tag{1}$$

Therefore, the $I_{LSP}^{\exp}(\theta)$ signal can be expressed as:

$$I_{LSP}^{\exp}(\theta)=k_1\cdot I_{LSP}(\theta), \tag{2}$$

$$I_{LSP}(\theta)=\frac{1}{2\pi}\int_0^{2\pi}\left[S_{11}(\theta,\varphi)+S_{14}(\theta,\varphi)\right]d\varphi, \tag{3}$$

where S_{11} and S_{14} are Mueller matrix elements [14], θ and φ are the polar and azimuthal angles, respectively, k_1 an instrumental calibrating coefficient.

In order to find a parametric function describing sub-micron structures behavior in light scattering two new operative quantities, J_{LSP} and J_{SSC}, will be introduced. They are integral quantities related, respectively, to forward and side scattering generated by the particle and detected by the photomultipliers. Integral forms have been selected because, even if in samples here analyzed aggregates are present more than single particles [15], structures with a diameter equal or smaller than 200 nm are supposed to be present and for such kind of particles the LSP signal intensity is low and S/N ratio is close to 1 [16]. The integral over a large angular range reduces the sensibility to the noise of the method.

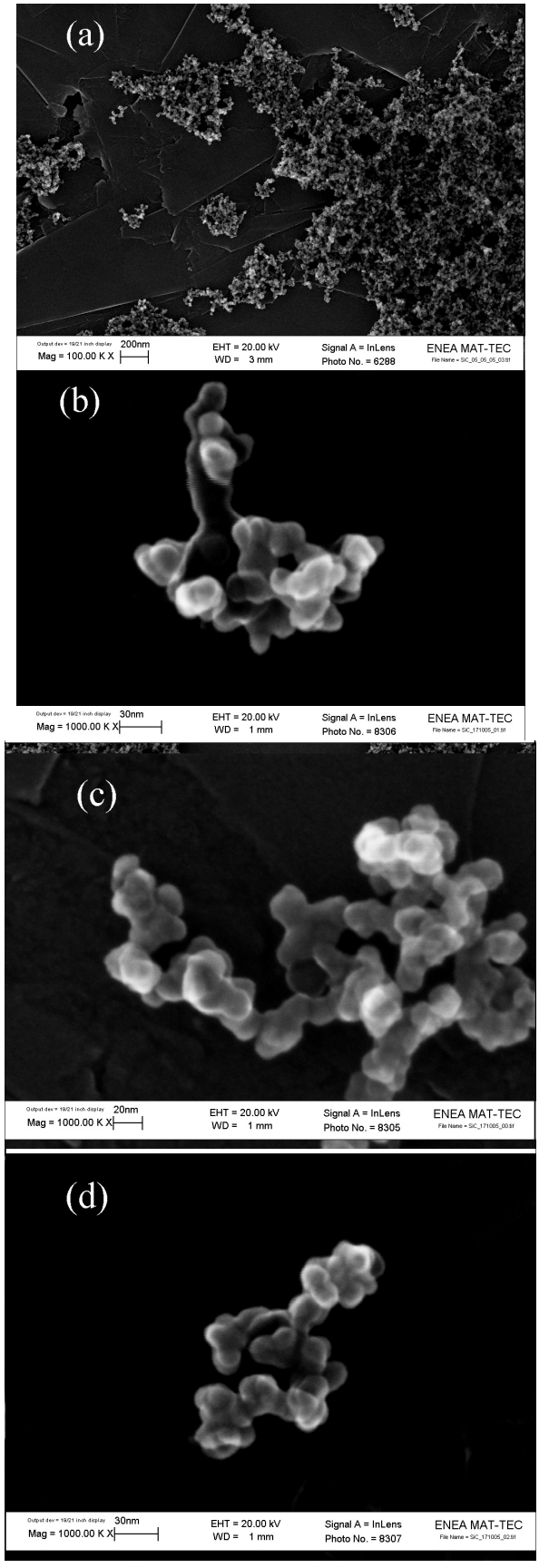

Fig. 2. SEM images of SiC nanoparticle aggregates; (a) is a general view of the sample; (b), (c) and (d) show single aggregates.

First the following LSP integral has been considered:

$$J_{LSP} = \int_{10}^{70} I_{LSP}^{\exp}(\theta)\sin^2\left(\frac{\pi}{60}(\theta - 10)\right)d\theta \qquad (4)$$

The integral is over all the reliable interval of measurement of LSP, starting at 10° and ending at 70°. Moreover the factor $\sin^2(\frac{\pi}{60}(\theta - 10))$ has been introduced in order to avoid the influence of angular range boundaries effects. In this way it is possible to reduce the influence of the high intensity band at the beginning and the noise at the end of the angular range.

With respect to the side scattering, the solid angle defined by Δθ and Δφ has been taken into account. The expression considered for this quantity is:

$$J_{SSC}^{\exp} = k_2 \cdot J_{SSC}, \qquad (5)$$

$$\mathrm{J_{SSC}} = \iint_{\frac{\pi}{2}\pm\frac{\Delta\theta}{2},\pm\frac{\Delta\varphi}{2}} [\mathrm{S_{11}}(\theta,\varphi) + \mathrm{S_{14}}(\theta,\varphi)]\sin(\theta)\mathrm{d}\theta\mathrm{d}\varphi \qquad (6)$$

Δθ and Δφ are the interval of integration over the polar and azimuthal angles, respectively. Values of Δθ and Δφ depend on the numerical aperture (NA) of the objective L_1. Since the objective used has NA equal to 0.30, then, in air the following relationship is valid:

$$\Delta\theta = \Delta\varphi = 2 \cdot \mathbf{arcsin}(0.3) = 34.9°.$$

k_2 represents an instrumental calibrating coefficient.

k_1 and k_2 have been determined as ratio of measured light scattering signals for 0.5 μm polystyrene microspheres averaged over 2000 beads and values calculated by (3) and (5) for sphere with diameter of 0.5 μm and refractive index of 1.6044 [17], assuming to work with a laser at 405 nm in water (n=1.34358). Under these conditions, the values retrieved for coefficients are $k_1 = 0.030$ and $k_2 = 0.378$.

2.3 Materials

In order to test the whole experimental LSFC apparatus and calibrate the measurements, polystyrene beads have been studied. Such spherical particles are characterized by certified diameters. In particular, the elements C (d=0.21 μm), D (d=0.5 μm), and E (d=0.11 μm) of carboxylate-modified microspheres F-8888 kit #2 Molecular Probes® have been used in our experiments.

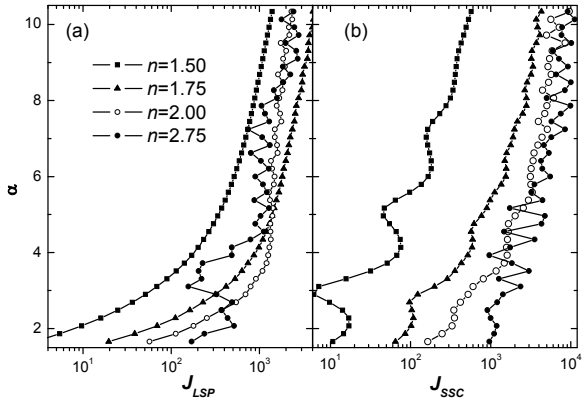

Fig. 3. Theoretical dependence of size parameter α of a sphere with d=0.50 μm on the integrals J_{LSP} and J_{SSC} for different refractive indices: 1.50, 1.75, 2.00 and 2.75.

As submicron structures to test the experimental apparatus and working method silicon carbide samples have been selected. In such samples SiC is disguised as aggregates of nanoparticles. The nanopowders analyzed in the present work were synthesized by laser assisted pyrolysis from gaseous precursors, namely SiH_4 and C_2H_2. The major advantage of this technique is the production of sizeable amount of nanopowders with mean size in the range 10-30 nm and a narrow size distribution [19]. The coalescence and growth of nanoparticles in the reaction plume occurs as a result of collisions between hot radicals and stops abruptly as soon as the particles leave the hot region. However, collisions between nanoparticles may still occur along the pathway to the collection system, giving rise to the formation of aggregates [10].

SEM images of the SiC samples under study (fig. 2) show the formation of SiC nanoparticle aggregates: chain like arrangements (with a mean size of 100 nm) of 20 nm sized particles connected by sintered necks can be observed. In particular, in fig. 2 (a) a general view of the sample in shown, while in fig. 2 (b), (c), (d) single aggregates are presented.

3. Results and discussion

Polystyrene microspheres have been used as calibration samples to verify the capability of LSFC to provide information on size of sub-micron structures.

Relationships between scattering parameters J_{LSP} and J_{SSC} and particles characteristics are needed to obtain size and refractive index values of particles. To find them we have compared, for polystyrene spheres, numerical simulations and LSFC experimental data.

In particular, by a conventional simulation program for Mie scattering, trends for the size parameter α (defined by α=d/λ, where d is the particle diameter and λ the laser wavelength) as a function of J_{LSP} and J_{SSC} have been studied for four different values of refractive index n (1.50, 1.75, 2.00, 2.75) and particle diameter (0.15, 0.50, 0.75, 1.00 μm). Results of such simulations for d=0.5 μm

and different refraction index n are reported in fig 3, where only homogeneous spheres have been taken into account. Here a good single-valued dependency of α can be noticed only on J_{LSP} for refractive indices from 1.50 to 1.75.

By these results the following particular parametric function has been selected to make a non-linear regression of experimental data on polystyrene microspheres, in fact their refractive index (n=1.6044) is inside the range for which there is the single-valued dependency.

$$\alpha = a \cdot J_{LSP}{}^{b} + c \tag{7}$$

where coefficient *a*, *b*, and *c* depend on refractive index. From the experimental results (fig. 4 shows some measured LPS signals of calibrated beads), the following values of the coefficients have been estimated for the refractive index of polystyrene, (n=1.6044, known from literature [17] for λ = 405 nm):

$a = 0.034 \pm 0.004$, $b = 0.691 \pm 0.012$, $c = 1.739 \pm 0.059$.

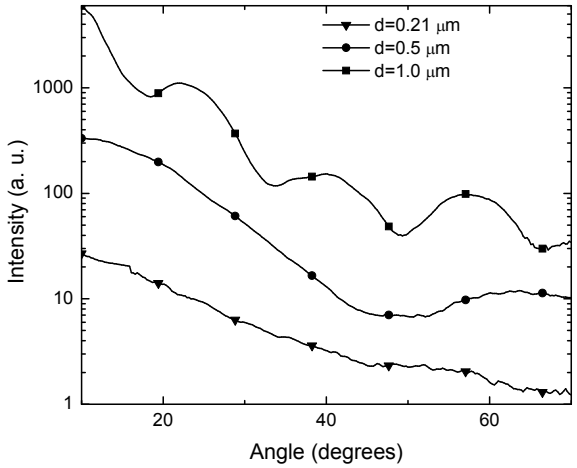

Fig. 4. Examples of forward light scattering experimental signals for polystyrene microspheres with d = 0.21 μm, 0.5 μm and 1.0 μm from bottom to top.

Then the size parameter α has been determined, in the range 1.60 - 10.40, from the eq. (7) with a mean square error σ = 0.11.

Therefore the empirical equation (7) has been applied to determine sizes of 0.2 μm and 0.5 μm sized polystyrene microspheres and the results are presented in tab.1. Despite the low S/N ratio experimentally obtained and the low relative accuracy in the zero level determination for experimental signals, a good agreement on mean size and standard deviation between Molecular Probes® datasheet and our data can be observed.

Unfortunately, the above relationships can not be used for SiC. In fact, the single-valued dependence exists only between α and J_{LSP} and only for refractive indices lower then n=1.70. In particular, for the refractive index of SiC (n=2.7621 [19]), the dependence of α on integrals J_{LSP} and J_{ssc} is not single-valued. But, anyway, a general increasing tendency of the size parameter with the integral values can be supposed to exist also for SiC nanoparticles aggregates.

Furthermore, the experimental LSP signals relative to SiC structures (see fig. 5) are not regular like the ones presented for polystyrene particles (fig. 4). Such different behavior is due to the fact that SiC nanoparticles in the aggregate forms are not arranged to generate a spherical shape (fig. 2).

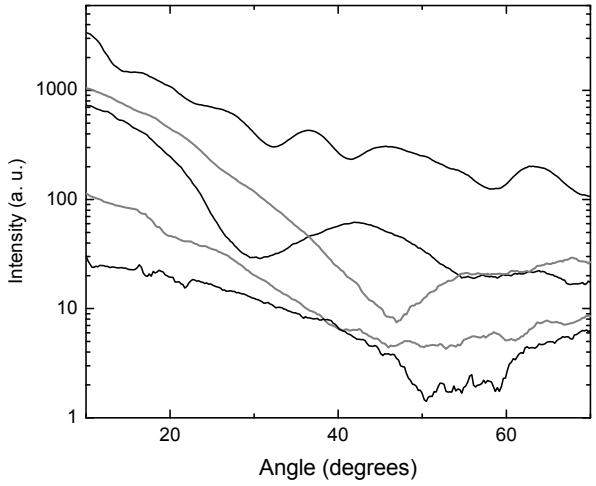

Fig. 5. Examples of forward light scattering signals for silicon carbide particles. Experimental data for 5 different SiC particles with unknown diameter are showed.

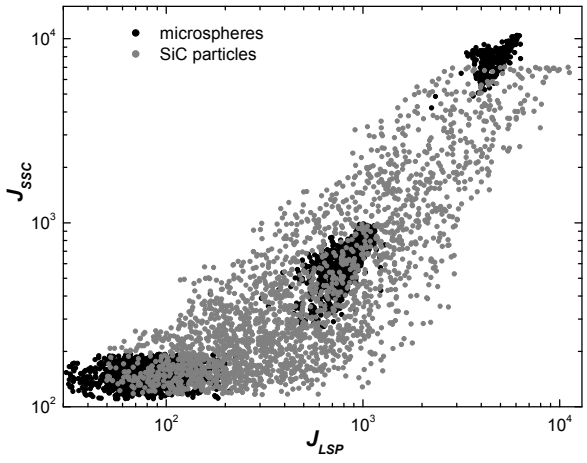

Fig. 6. Experimental biparametric diagram of integral of side scattering J_{ssc} versus integral of LSP J_{LSP} for polystyrene microspheres (black dots) and for silicon carbide particles (gray dots).

However, despite such difficulties, a comparison among experimental data on J_{LSP} and J_{SSC} can be a tool to distinguish different kinds of samples and to generically

characterize them directly from measurements without additional calculations. In fact, as it is possible to notice from fig. 6, experimental points referring to SiC and polystyrene can be found, mainly, in different areas of the biparametric diagram, where latex beads are located in three well known area, SiC are spread over all.

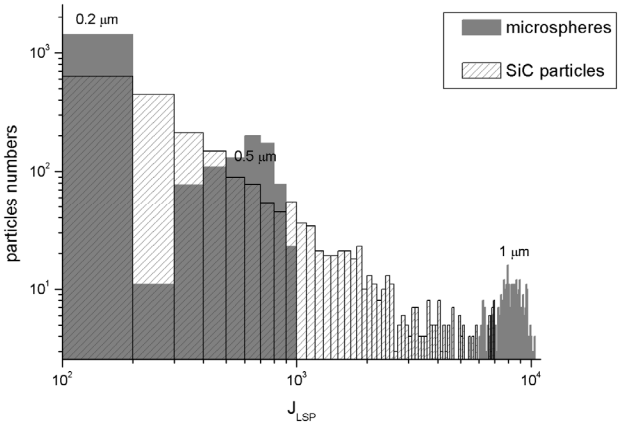

Fig. 7. Experimental distribution of J_{LSP} for SiC sample and for polystyrene microspheres with d=1, 0.5, 0.2, μm.

Moreover, the experimental distribution of J_{LSP} showed in fig. 7 can offer an idea of the sample size distribution by means of the comparison to the distributions for calibrated spheres. The graph suggests us that the majority of the aggregates analyzed has $d \leq 0.2$ μm, but the distribution has a tail up to 1 μm.

LSFC results have been compared to data coming from a more conventional instrument based on light scattering detection, as DLS is. With this aim, the same SiC samples analyzed by LSFC (suspensions in pure distilled water) have been studied by a DLS MALVERN PCS 4700. The Z average obtained for the size distribution resulted to be 1633.6 ± 60.8 nm. The large difference between this value and the LSFC results, shown in fig. 7 and described above, (even if only indicative) can be easily explained by difficulties DLS encountered measuring this kind of sample. In fact, it is not a typical sample for which DLS provide good results [20]: it has a very large size distribution and particles have the tendency to precipitate, i.e. they do not undergo only the Brownian motion. Therefore a real comparison on data could not be made, but it is possible to highlight how where DLS is not able to provide reliable data, LSFC gives size distribution (see fig. 7), although rough.

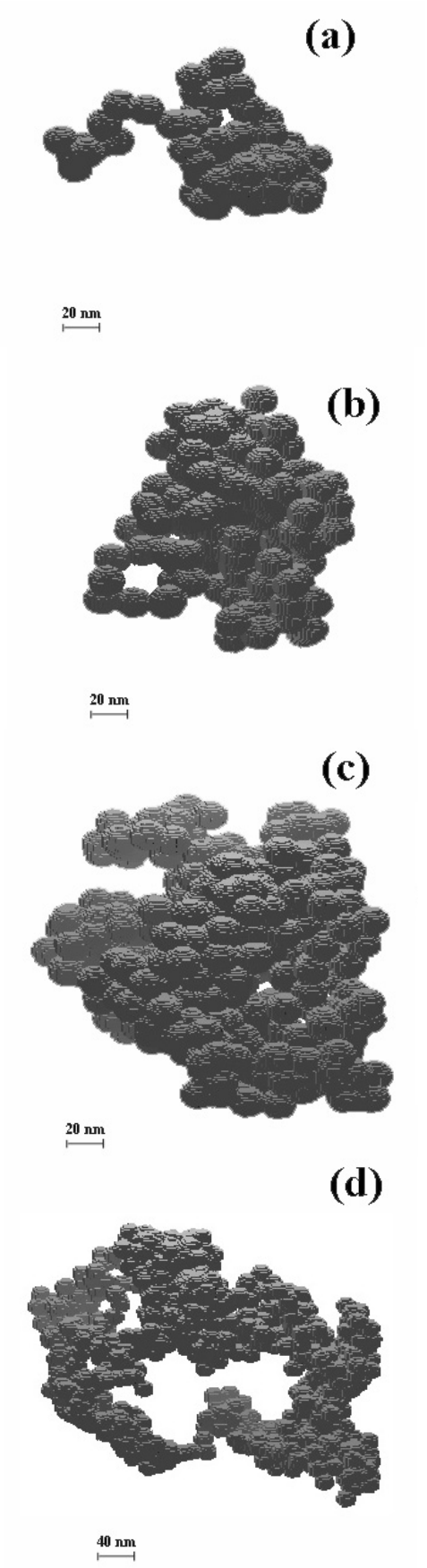

Fig. 8. Models of SiC nanoparticle aggregates for light scattering simulation with volume - equivalent size: 0.17 μm (a), 0.22 μm (b), 0.27 μm (c), 0.37 μm (d).

Another way to verify the validity of LSFC results was based on light scattering simulation on SiC aggregates models. To this purpose, four different three-dimensional models of SiC aggregates have been built. Such models represent four real structures randomly chosen among structure in SEM images of the sample recorded and are constituted by sets of spheres with diameters of 20 nm joined together in an arbitrary order. 3D images of the models are depicted in fig. 8.

The Discrete Dipole Approximation (DDA) approach has been applied for calculations on the SiC aggregates models [18]. In fact, DDA is a general method to simulate light scattering by arbitrary shaped particles. Such structures can be very far from spherical shape. For this reason, in order to define them from a dimensional point of view, the value of the equivalent-volume size is used. The latter is the diameter that a sphere with the volume of the particle modeled would have. DDA simulations have been carried out on Netherlands National Compute Cluster LISA [19]. Fig. 9 shows the LSP of modeled particles; letters (a), (b), (c) and (d) correspond to shapes presented on fig. 8 and have the following equivalent-volume sizes: 0.17 μm (a), 0.22 μm (b), 0.27 μm (c), 0.37 μm (d). For every structure, the LSPs depend on relative orientation of the incident beam. For the present work, arbitrary orientations have been selected for light scattering simulations. An increase of the LSP mean value with the equivalent-volume size can be noticed.

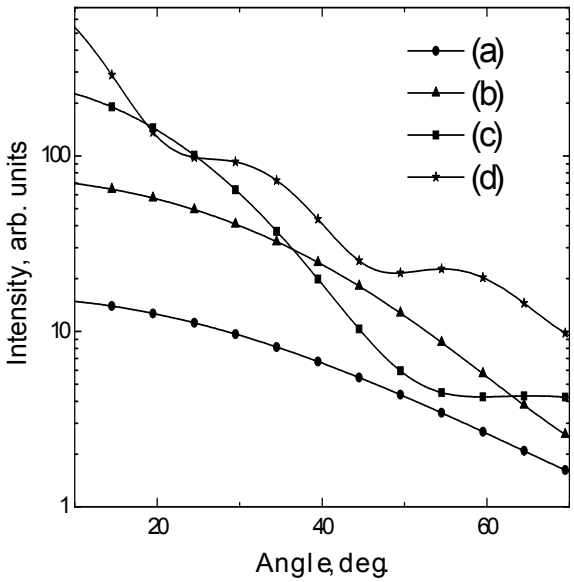

Fig. 9. LSPs of SiC nanoparticle aggregates models presented on fig. 7.

The simulated light scattering integrals J_{SSC} and J_{LSP} for modeled particles (a), (b), (c) and (d) are presented on the biparametric diagram of fig. 10. The black line contour is boundary of measured SiC particles. The integrals J_{SSC} and J_{LSP} of particles (a), (b), (c) are within this contour but particles (d). The location of the integrals within the delimited area means that our modeled particles are close to real particles. Conversely, the integral that results outside of the contour can suggest that, in the simulation, the orientation of the particle with respect to the incident beam differs from the real orientation. Another reason of such a result can be, however, related to the presence of a hole in the structure (d), that makes it particularly far from a regular shape.

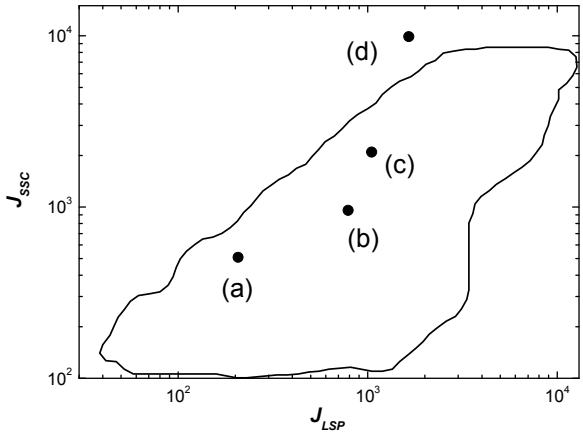

Fig. 10. Biparametric diagram of integral of side scattering J_{ssc} versus integral of LSP J_{LSP} for SiC nanoparticle aggregates models and boundaries of experimental data distribution from fig. 6.

The results of the model, therefore, confirm the validity of the scanning flow cytometry as analysis method to retrieve size information on single non-spherical sub-micron particles, that can be hardly characterized by classical technique as DLS or SEM, both for the difficulty in obtaining relevant data from the statistical point of view and for the large size distribution that such kind of samples can have.

4. Conclusions

In the present work we have analyzed sub-micron particles by a Laser Scanning Flow Cytometer equipped with two channels, for side scattering and forward scattering in a wide angular range, between 10° and 70° . At first, polystyrene calibrated spheres have been used to test the capabilities of the experimental apparatus and of the developed algorithms. Then samples of SiC aggregates have been taken into account. Despite the difficulties in measuring sub-micron particles with irregular shapes, a size distribution for such sample has been obtained and a way to distinguish different kinds of particles has been provided.

DDA simulations on SiC nanostructure aggregate models have shown results very close to the experimental ones, even if the studied particles present shapes far from

spherical. Such agreement confirms the quality of the experimental method here tested.

In conclusion, good results obtained on polystyrene 0.2 and 0.5 μm beads and SiC samples demonstrate that SFC turns out to be an useful measurement tool also for non-spherical aggregates with dimensions lower than 1 μm. In fact, it can provide size distribution and statistics on a large amount of particles, studied individually. Such characteristics make the LSFC a technique with unique properties, compared to classical analysis methods, as SEM and DLS, that supply as results mean values or not statistically relevant data.

Acknowledgements

The authors would like to thank Mariano Carpanese and Fabio Fabbri (ENEA, FIM-FISLAS), for SiC aggregates production; Emanuele Serra (ENEA, FIM-MATTEC) for Transmission Electron Microscopy imagery; Mauro Falconieri for DLS measurements. Furthermore, we are deeply grateful to Elisabetta Borsella for her involvement.

References

[1] A. V. Chernyshev, V. I. Prots, A. A. Doroshkin, V. Maltsev Appl. Optics **34**, 6301(1995).
[2] E. H. Piepmeier (1986) Analytical Applications of lasers, Laser flow cytometry, Wiley Interscience ed., p. 521
[3] V. P. Maltsev, Lopatin VN Appl. Optics **36**, 6102 (1997).
[4] M. R. G. O'Gorman Clinics in laboratory medicine **27**, 591(2007).
[5] Z. Ulanowski, R. S. Greenaway, P. H. Kaye, I. K. Ludlow Meas. Sci. Technol. **13**, 292 (2002)
[6] P. J. Wyatt Instrum. Sci. Technol. **25**, 1(1997).
[7] P. J. Wyatt, D. T. Phillips Theor. Biosci. **37**, 493 (1972).
[8] K. Semyanov, V. P. Maltsev Part Part Syst Char **17**, 225 (2000).
[9] J. Y. Fan, X. L. Wu, P. K. Chu Prog. in Mater. Sci. **51,** 983 (2006).
[10] W. H. Marlow (2004) in "Gas phase nanoparticle synthesis", Kluwer Academic Publisher, p.1
[11] A. E. Gunnaes, A. Olsen, A. Skogstad J. Mater. Sci. **40**, 6011(2005).
[12] B. J. Berne, R .Pecora Dynamic light scattering, John Wiley & Sons, New York (1976).
[13] F. Barnaba, L. Fiorani, A. Palucci, P. Tarasov Journal of Quant. Spectrosc. Ra. **102**, 11(2006).
[14] R. Guenther Modern optics, ed. Wiley, New York (1990).
[15] E. Müller, R. Dittrich, E. Borsella, M. Carpanese Proceed. NANO 2004 Wiesbaden (Germania) ed. Dechema EV, p. 29 (2004).
[16] K. A. Semyanov, P. A. Tarasov, A. E. Zharinov, A. V. Chernyshev, A. G. Hoekstra, V. P. Maltsev, Appl. Optics **43**: 5110 (2004)
[17] X. Ma, J. Q. Lu, R. S. Brock, K. M. Jacobs, P. Yang, X. H. Hu Phys. Med. Biol. **48**, 4165 (2003).
[18] S. O. Konorov, D. A. Sidorov-Biryukov, I. Bugar, J. Kovac, L. Fornarini, M. Carpanese, M. Avella, M. E. Errico, D. Chorvat, J. Kovac, R. Fantoni, D. Chorvat, A. M. Zheltikov Appl. Phys. B **78**, 73 (2004).
[19] P.T.B. Shaffer Appl. Optics **10**, 1034 (1971).
[20] R. D'Amato, I. Venditti, M. V. Russo, M. Falconieri, J. Appl. Pol. Sci. **102,** 4493(2006).
[21] M. A. Yurkin, A. G. Hoekstra J. Quant. Spectrosc. Ra. **106**, 558 (2007)
[22] http://www.sara.nl/userinfo/lisa/.

*Corresponding author: spizzich@frascati.enea.it